Table IV. Selected Atomic Positional (×10⁴) and Thermal (×10³) Parameters for **2**

atom	*x*	*y*	*z*	*U*, Å²[a]
Rh	7455.0 (4)	7006.9 (2)	3116.5 (4)	28.2 (2)*
Co	8387.8 (7)	7214.5 (4)	5645.3 (7)	27.5 (3)*
P(1)	7688 (1)	8219 (1)	3270 (1)	30 (1)*
P(2)	7818 (1)	5934 (1)	3004 (1)	31 (1)*
P(3)	9326 (1)	6433 (1)	5937 (1)	28 (1)*
P(4)	9155 (1)	8414 (1)	6153 (1)	28 (1)*
H(1)	8918 (45)	7347 (25)	4717 (44)	21 (13)
C(10)	9179 (5)	8775 (3)	4788 (5)	33 (1)
C(20)	9343 (5)	6091 (3)	4482 (5)	32 (1)
C(1)[b]	6247 (13)	6701 (7)	1359 (12)	36 (3)
O(1)[b]	5469 (10)	6521 (5)	301 (9)	62 (3)
C(1a)[b]	6562 (17)	6856 (10)	1327 (17)	31 (5)
O(1a)[b]	5939 (14)	6731 (8)	229 (13)	58 (4)
C(2)	6693 (6)	6813 (3)	4507 (6)	35 (1)
O(2)	5602 (4)	6568 (2)	4117 (4)	51 (1)
C(3)	8437 (6)	7213 (3)	7102 (6)	41 (1)
O(3)	8481 (5)	7210 (3)	8090 (5)	66 (1)

[a] Parameters marked with an asterisk denote atoms assigned anisotropic thermal parameters given as the isotropic equivalent displacement parameter defined as $U_{eq} = {}^1/_3\sum_i\sum_j U_{ij}a^*_i a^*_j a_i a_j$. [b] Occupancy (1)/(1a) = 0.6/0.4.

tation matrix were determined from a least-squares treatment of 20 accurately centered high-angle reflections ($26.0 < 2\theta < 30.0°$).[10] Intensity data of 9133 reflections were collected in the range $0 < \theta < 25°$, in ω–2θ mode, at variable scan speeds (1.37–2.75 deg min⁻¹) and scan width of 0.8 + 0.35 tan θ, with a maximum time per datum of 60 s. Standard reflections of 00$\bar{1}$, 020, and 200 were monitored every 180 min of X-ray exposure time and showed 2.3% random decay over the total period of 130.7 h. Corrections were made for Lorentz, monochromator and crystal polarization, background radiation effects but not for decay using the Structure Determination Package[11] running on a PDP 11/23+ computer. An empirical absorption correction was applied[12] using a 360° ψ-scan for nine reflections in the range $1.97 < \theta < 14.84°$. The cell parameter and systematic absences indicated[13a] that the space group was $P2_1/c$ and the correctness of the choice of the space group was confirmed by successful solution and refinement of the structure. The structure was solved with MULTAN[14] and subsequent difference Fourier techniques. Refinement on F was carried out by full-matrix least-squares techniques using the SHELX-76 software[15] running on a SUN 3/80 workstation. Scattering factors for neutral, non-hydrogen atoms were taken from ref 13b. Anisotropic thermal parameters were assigned for Rh, Co, and P atoms and were refined, while the thermal parameters of all the remaining non-hydrogen atoms were refined isotropically. The hydrogen atoms attached to the carbon atoms were introduced on calculated positions (C–H = 0.90 Å) and were included in the refinement riding on their carrier atoms. The hydride atom was located from a difference Fourier map unambiguously, and the positional and thermal parameters were refined in the least-squares cycles. The disorder in the BF_4^- anion was successfully resolved. With the use of 6160 observations with $I > 3\sigma(I)$ and the use of weights of the form $w = k/\sigma^2(F_o) + gF^2$ where $k = 2.2259$ and $g = 0.000\,606$, refinement of 219 variables converged at agreement factors $R = 0.0519$ and $R_w = 0.0558$. The top five peaks in the final difference Fourier synthesis with electron density in the range 0.805 to 0.712 e Å⁻³ and are associated with O(3), C(315), C(313), F(2), and C(215) at distances 0.57–0.78 Å. The experimental details and crystal data and selected positional and U(equiv) thermal parameters are given in Tables III and IV. Selected bond distances and angles are collected in Table I. More complete tables and tables of anisotropic thermal parameters, calculated hydrogen atom positional parameters, root-mean-square amplitudes of vibration, weighted least-squares planes and dihedral angles, selected torsion angles, and structure amplitudes have been deposited as supplementary material.

Acknowledgment. We thank the NSERC (Canada) for financial support and Dr. N. C. Payne for X-ray facilities.

Supplementary Material Available: A summary of the X-ray structure determination and tables of crystallographic data, atomic positional and thermal parameters, bond distances and angles, hydrogen atom positional parameters, least-squares planes, and torsion angles for **2** (9 pages); a table of observed and calculated structure factors for **2** (37 pages). Ordering information is given on any current masthead page.

(10) *CAD4 Diffractometer Manual*; Enraf-Nonius: Delft, The Netherlands, 1988.
(11) Enraf-Nonius Structure Determination Package, SDP-PLUS, Version 3.0. 1985.
(12) North, A. C. T.; Phillips, D. C.; Mathews, R. S. *Acta Crystallogr., Sect. A* **1968**, *24*, 351.
(13) *International Tables for X-ray Crystallography*: (a) Vol. A, D. Reidel Publishing Co.: Boston, MA, 1983; (b) Vol. IV, Kynoch Press: Birmingham, England, 1974.
(14) Main, P. MULTAN 82 Manual. 1982.
(15) Sheldrick, G. M. SHELX-76. Program for Crystal Structure Determination. University of Cambridge, England, 1976.

Contribution from the Department of Chemistry, University of Missouri—Kansas City, Kansas City, Missouri 64110

Electronic Structure Calculations on Octanuclear Silsesquioxanes and Aluminosilsesquioxanes

Clarke W. Earley

Received August 8, 1991

Semiempirical electronic structure calculations have been performed on a series of octanuclear molecular silicates and aluminosilicates to determine the effects of substitution of tetravalent silicon by trivalent aluminum. By inclusion of molecular species that have already been isolated and characterized, these calculated results have been compared directly with experimental values to determine the reliability of the results obtained. Although these calculations consistently predict Si–O bonds to be slightly longer than observed experimentally, they are shown to be quite successful at reproducing geometric trends within a related series of molecules. The calculated relative stabilities for compounds containing two or more aluminum atoms predict that isomers containing Al–O–Al linkages should be thermodynamically less stable, consistent with Loewenstein's rule for solid-state aluminosilicates. Selected studies of monoprotonated species have also been performed to determine the relative stability of different protonation sites, especially with regard to the proximity to aluminum. As expected, protonation of bridging oxygen atoms near trivalent aluminum sites is predicted to result in thermodynamically more stable, and thus less acidic, species than those produced by protonation of oxygen atoms bridging two tetravalent silicon atoms.

Introduction

Zeolites are aluminosilicates characterized by a framework structure containing open channels and cavities of molecular dimensions. They have found a number of industrial uses as adsorbents, ion-exchangers, and shape-selective catalysts. A variety of both naturally-occurring and synthetic zeolites are known, spanning a range of structural and physical properties. The physical properties of zeolites are known to be strongly dependent on the structure and composition of atoms present, and a large number of studies of zeolite structures and properties have

0020-1669/92/1331-1250$03.00/0

appeared.[1] The relatively recent accessibility of a number of powerful characterization techniques, most notably solid-state magic angle spinning ^{29}Si FT-NMR spectroscopy,[2] has lead to considerable advances in the understanding of zeolite chemistry.

In 1954, Loewenstein proposed[3] that the formal substitution of aluminum for silicon in aluminosilicates was not an entirely random process but instead was governed by the restriction that aluminum atoms should not occupy adjacent tetrahedral sites. This premise accounted for several previously observed phenomena and has since been supported by a number of experimental studies.[4] Discontinuities in unit cell parameters for zeolites spanning a range of Al/Si ratios led Dempsey to propose[5] that secondary interactions between aluminum atoms (Al–O–Si–O–Al) should also be minimized. While recent work suggests that the number of these secondary interactions is not always completely minimized,[6] there is clear evidence that aluminum substitution patterns are more ordered than required based solely on Loewenstein's rule.

A large number of theoretical studies examining different aspects of zeolite chemistry have appeared, which can be divided into two predominate computational approaches. The first has been to use high-level ab initio calculations on small molecular silicates and aluminosilicates.[7] While this type of calculation holds the promise of a high degree of accuracy and is becoming more accessible due to increases in computational power, ab initio programs are computationally intensive and are still limited to relatively small systems. This has typically limited systematic investigations using this approach to systems containing three or fewer second-row (silicon, aluminum, and/or phosphorus) atoms. A second approach has been to apply molecular mechanics and dynamics calculations[8] to model zeolites. As these calculations are much less computationally-demanding, they can be performed on much larger systems, which should more closely approximate the solid-state structures of zeolites. Molecular mechanics approaches are especially well suited for studying the relative energetics of different geometries and have been used to compare the relative stability of different zeolite frameworks.[7b,8a] One disadvantage of this second approach is that it is not quantum mechanical in nature and therefore cannot be used to explain electronic effects. This is an especially important limitation if reaction mechanisms or the relative acidity/basicity of different sites is to be examined. Recently, a hybrid approach has been used in which a selected set of atoms is placed within a fixed 3-dimensional lattice of point charges (corresponding to an optimized zeolite lattice), and these selected atoms are then treated using ab initio calculations.[9]

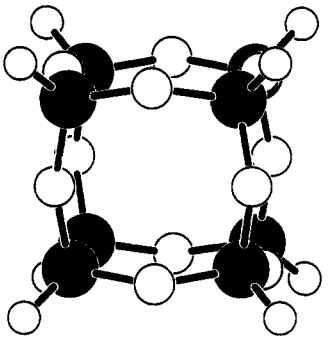

Figure 1. Schematic illustration of $H_8Si_8O_{12}$. In this figure, the large filled spheres represent silicon centers, the large open spheres represent the bridging oxygen atoms, and the small open spheres represent the terminal hydrogen atoms.

The goal of the present work is to use semiempirical quantum mechanical calculations to examine the relative stability of molecular aluminosilicate structural isomers in an effort to understand substitution patterns in aluminosilicates. Semiempirical methods are approximations to Hartree–Fock theory in which only valence shell orbitals are included and the most time-consuming integrals are either ignored or replaced by parametrized functions.[10] Although semiempirical calculations are a quantum mechanical approach, they offer little benefit for study of smaller systems that can be treated using more rigorous methods due to the inherent limitations of the approximations used. The real advantage of semiempirical calculations comes when they are applied to systems that are simply too large to be treated using ab initio methods. In this work, semiempirical calculations using the AM1 Hamiltonian[11] are performed on molecules of sufficient size to allow relatively long-range effects to be examined. A few studies using semiempirical calculations to examine larger silicates have been reported.[12]

The system chosen for initial studies is based on the octanuclear silsesquioxane $H_8Si_8O_{12}$ shown in Figure 1. These molecules are completely analogous to the double four-rings found as the "secondary building unit"[13] of zeolites having the Linde Type A (LTA) structure.[14] The four-membered rings in these molecules are constrained to be much more rigid than cyclic molecules, which should therefore make these molecules closely related to the four-rings found in a number of different zeolites. Finally, a number of molecules containing this Si_8O_{12} core have been synthesized[15] and have potential uses as precursors for the preparation

(1) For recent general reading on zeolites, see (a) Dyer, A. *An Introduction to Zeolite Molecular Sieves*; Wiley: New York, 1988. (b) *Zeolites: Facts, Figures, Future*; Jacobs, P. A., van Santen, R. A., Eds.; Elsevier: Amsterdam, 1989. (c) Szostak, R. *Molecular Sieves: Principles of Synthesis and Identification*; Van Nostrand Reinhold: New York, 1989. (d) *Introduction to Zeolite Science and Practice*; Bekkum, H., Flanigen, E. M., Jansen, J. C., Eds.; Elsevier: Amsterdam, 1991.

(2) For a review of application of MAS-NMR to determination of zeolite structure, see: Fyfe, C. A.; Thomas, J. M.; Klinowski, J.; Gobbi, G. C. *Angew. Chem., Int. Ed. Engl.* **1983**, *22*, 259–336.

(3) Loewenstein, W. *Am. Mineral.* **1954**, *39*, 92–96.

(4) For example, see: Bennett, J. M.; Blackwell, C. S.; Cox, D. E. In *Intrazeolite Chemistry*; Stucky, G. D., Dwyer, F. G., Eds.; ACS Symposium Series 218; American Chemical Society: Washington, DC, 1983; pp 143–158.

(5) Dempsey, E.; Kuhl, G. H.; Olson, D. H. *J. Phys. Chem.* **1969**, *73*, 387–390.

(6) Herrero, C. P. *J. Phys. Chem.* **1991**, *95*, 3282–3288.

(7) (a) Gibbs, G. V., G. V.; Meagher, E. P.; Newton, M. D.; Swanson, D. K. In *Structure and Bonding in Crystals*; O'Keeffe, M.; Navrotsky, A., Eds.; Academic Press: New York, 1981; Vol. 1, pp 195–225. (b) van Santen, R. A.; Ooms, G.; den Ouden, C. J. J.; van Beest, B. W.; Post, M. F. M. In *Zeolite Synthesis*; Occelli, M. L., Robson, H. E., Eds.; ACS Symposium Series 398; American Chemical Society: Washington, DC, 1989; pp 617–633. (c) Pelmenshchikov, A. G.; Paukshtis, E. A.; Stepanov, V. G.; Pavlov, V. I.; Yurchenko, E. N.; Ione, K. G.; Zhidomirov, G. M.; Beran, S. *J. Phys. Chem.* **1989**, *93*, 6725–6730. (d) Sauer, J. *Chem. Rev.* **1989**, *89*, 199–255. (e) Derouane, E. G.; Fripiat, J. G.; von Ballmoos, R. *J. Phys. Chem.* **1990**, *94*, 1687–1692.

(8) (a) Ooms, G.; van Santen, R. A.; Jackson, R. A.; Catlow, C. R. A. In *Innovations in Zeolite Materials Science*; Grobet, P. J., Mortier, W. J., Vansant, E. F., Schulz-Ekloff, G., Eds.; Elsevier: Amsterdam, 1988; pp 317–322. (b) Demontis, P.; Yashonath, S.; Klein, M. L. *J. Phys. Chem.* **1989**, *93*, 5016–5019. (c) Titiloye, J. O.; Parker, S. C.; Stone, F. S.; Catlow, C. R. A. *J. Phys. Chem.* **1991**, *95*, 4038–4044. (d) Nicholas, J. B.; Hopfinger, A. J.; Trouw, F. R.; Iton, L. E. *J. Am. Chem. Soc.* **1991**, *113*, 4792–4800.

(9) (a) Vetrivel, R.; Catlow, C. R. A.; Colbourn, E. A. *J. Phys. Chem.* **1989**, *93*, 4594–4598. (b) Vetrivel, R.; Catlow, C. R. A.; Colbourn, E. A.; Leslie, M. In *Zeolites as Catalysts, Sorbents and Detergent Builders*; Karge, H. G., Weitkamp, J., Eds.; Elsevier: Amsterdam, 1989; pp 409–419. (c) Vetrivel, R.; Catlow, C. R. A.; Colbourn, E. A. In *Zeolites: Facts, Figures, Future*; Jacobs, P. A., van Santen, R. A., Eds.; Elsevier: Amsterdam, 1989; pp 795–803.

(10) (a) Pople, J. A.; Beveridge, D. L. *Approximate Molecular Orbital Theory*; McGraw-Hill: New York, 1970. (b) Klopman, G.; Evans, R. C. In *Semiempirical Methods of Electronic Structure Calculation; Part A: Applications*; Segal, G. A., Ed.; Plenum Press: New York, 1977.

(11) Dewar, M. J. S.; Zoebisch, E. G.; Healy, E. F.; Stewart, J. J. P. *J. Am. Chem. Soc.* **1985**, *107*, 3902–3909.

(12) (a) Carson, R.; Cooke, E. M.; Dwyer, J.; Hinchliffe, A.; O'Malley, P. J. In *Zeolites as Catalysts, Sorbents, and Detergent Builders*; Karge, H. G., Weitkamp, J., Eds.; Elsevier: Amsterdam, 1989; pp 39–48. (b) Mortlock, R. F.; Bell, A. T.; Chakraborty, A. K.; Radke, C. J. *J. Phys. Chem.* **1991**, *95*, 4501–4506.

(13) Meier, W. M.; Olson, D. H. *Atlas of Zeolite Structure Types*; Butterworth: Stoneham, MA, 1988.

(14) For crystal structure determinations of zeolites having the LTA structure, see: (a) Howell, P. A. *Acta Crystallogr.* **1960**, *13*, 737–741. (b) Leung, P. C. W.; Kunz, K. B.; Seff, K.; Maxwell, I. E. *J. Phys. Chem.* **1975**, *79*, 2157–2162. (c) Vance, T. B.; Seff, K. *J. Phys. Chem.* **1975**, *79*, 2163–2167.

of novel materials. Since the calculational studies have actually been performed on molecular silicates and aluminosilicates, it should be possible to use these results to explain some of the features of molecules that have already been isolated and characterized[16] and predict the properties and relative stabilities of selected "target" molecules. Perhaps more importantly, the experimental results can be used to ascertain the absolute accuracy/reliability of the theoretical results obtained in this work.

There are several advantages to examining a series of aluminosilicates of this size (or larger). The first is that a relatively large number of structural isomers can be examined containing several different Si/Al ratios. While the energetic effects of having two or more adjacent aluminum atoms can be examined using smaller systems, study of larger systems is required for examination of long-range substitution patterns. To illustrate this point, consider a model calculation to examine the rather short-range interaction controlled by Loewenstein's rule. The smallest aluminosilicates having different isomers that may or may not contain Al–O–Al linkages is a three-membered chain ($R_8Al_2SiO_2$) or a four-membered ring ($R_8Al_2Si_2O_4$). Obviously, to examine longer-range effects (such as the "next-nearest neighbor" interactions referred to by Dempsey's rule) requires larger systems. Finally, it is expected that silsesquioxanes should be better models for zeolites than either chains or single-ring molecules since silsesquioxanes (μ-O/Si = 1.5) come much closer to the ideal ratio of bridging oxygen to silicon sites (μ-O/Si = 2.0) than either chains (μ-O/Si < 1.0) or rings (μ-O/Si = 1.0). Octanuclear cubes were chosen for examination in this work since they are the smallest silsesquioxane "building blocks" found in zeolite structures.[17]

Methodology

All calculations employ the semiempirical AM1 Hamiltonian[11] as implemented in the program AMPAC[19] using standard literature values for all parameters.[20] Calculations were performed on molecules with the general formula $H_yR_8Al_xSi_{8-x}O_{12}^{(x-y)-}$ (R = H, OH; x = 0–4; y = 0–1). All possible isomers containing y = 0 (unprotonated) were examined as were selected protonated species (y = 1). All geometric parameters were fully optimized without any symmetry constraints for each structure and force calculations[21] performed to verify that the final geometries obtained were minima. Complete tables of optimized geometries and calculated atomic charges are included as supplementary material. Partial charges and bond orders were calculated using the default analysis procedure contained in the AMPAC program, which uses a Coulson density matrix.[22] In this procedure, the occupany of each atomic orbital is calculated by summing the squares of the normalized atomic orbital basis set coefficients and multiplying by the occupancy of each molecular orbital. The partial charge is then obtained by subtracting the sum of these occupancies from the number of valence electrons on each atom. Bond orders are calculated by summation of the squares of appropriate off-diagonal elements of the density matrix.

Table I. Comparison of Experimental and Calculated Geometries of Silicates

	Si–O, Å		Si–O–Si, deg		
molecule	calcd[a]	exptl	calcd[a]	exptl	ref
$H_3Si–O–SiH_3$	1.725[b]	1.634	154[b]	144	*c*
$H_8Si_8O_{12}$	1.709	1.619	155	148	*d*
$(CH_3)_8Si_8O_{12}$	1.712	1.61	156	145	*e*
$(CH_3O)_8Si_8O_{12}$	1.703	1.604	156	148	*f*
$(C_6H_5)_8Si_8O_{12}$		1.612		149	*g*
$(C_6H_5CH_2)_8Si_8O_{12}$		1.616		149	*h*

[a] This work. [b] Dewar, M. J. S.; Jie, C. *Organometallics* **1987**, *6*, 1486–1490. [c] Almenningen, A.; Bastiansen, O.; Hedberg, K.; Tretteberg, M. *Acta Chem. Scand.* **1963**, *17*, 2455. [d] Heyde, T. P. E.; Burgi, H. B.; Burgy, H.; Tornroos, K. W. *Chimia* **1991**, *45*, 38–40. [e] Larsson, K. *Arkiv Kemi* **1960**, *16*, 203–208. [f] Day, V. W.; Klemperer, W. G.; Mainz, V. V.; Millar, D. M. *J. Am. Chem. Soc.* **1985**, *107*, 8262. [g] Hossain, M. A.; Hursthouse, M. B.; Malik, K. M. A. *Acta Crystallogr.* **1979**, *B35*, 2258. [h] Feher, F. J.; Budzichowski, T. A. *J. Organomet. Chem.* **1989**, *373*, 153–163.

Results and Discussion

Calculated Geometries. One of the first requirements of any computational study is to verify that the method(s) used is able to provide results in acceptable agreement with the properties one is trying to determine. A comparison of the calculated geometries obtained in this work with the available experimental data for a number of molecular silicates is summarized in Table I. From these results, it is apparent that the calculated Si–O bond lengths are consistently too long by ca. 0.10 Å and the calculated Si–O–Si angles are too large by ca. 10°. While these errors are somewhat larger than one would like, they are still within acceptable agreement with experiment. The potential energy surface of the Si–O–Si linkage is known to be unusually flat,[7a] and accurate determination of Si–O bond lengths and Si–O–Si angles in these types of molecules requires high levels of theory.[23] An encouraging feature of these results is that the differences between the calculated and observed values for H_6Si_2O and the $R_8Si_8O_{12}$ molecules remains reasonably constant, suggesting that the errors are predominantly size independent. This is under investigation as work on larger systems is currently in progress.

Examination of the experimental geometries presented in Table I suggests that alkyl/aryl substituents on the corners of the cube result in slightly longer (0.006–0.012 Å) Si–OSi bonds than those observed when an alkoxide group is present, although drawing this type of conclusion based on a single crystal structure containing an alkoxide substituent is tenuous at best. However, the calculated Si–OSi bond lengths in $(HO)_8Si_8O_{12}$ and $(CH_3O)_8Si_8O_{12}$ are virtually identical (1.703 Å) and shorter by 0.009 Å than those calculated for $(CH_3)_8Si_8O_{12}$, which is consistent with this suggestion.

The average calculated Si–OH bond lengths in $(HO)_8Si_8O_{12}$ is 1.728 Å, or about 0.025 Å longer than the average Si–OSi bond lengths. While the absolute bond lengths are again too long, the calculated bond *lengthening* is in reasonable agreement with that observed in the X-ray structural determination of $Cy_7Si_7O_9(OH)_3$ (Cy = cyclohexyl) by Feher et al.[18] In this structure, these workers found that Si–OSi bond lengths averaged 1.608 Å and the three Si-OH bond lengths averaged 1.622 Å.

The X-ray crystal structure of an aluminosilicate, $(Ph_3PO)(C_6H_{11})_7AlSi_7O_{12}$, has recently been determined.[24] In this structure, the Si–OSi bond lengths were found to range from 1.609 to 1.631 Å while the Si–OAl bonds ranged from 1.593 to 1.595 Å. The three Al–OSi bonds ranged from 1.714 to 1.719 Å. The Si–O bond lengths calculated in the present work for

(15) (a) Wiberg, E.; Simmler, W. *Z. Anorg. Allg. Chem.* **1955**, *282*, 330–344. (b) Brown, J. F. *J. Am. Chem. Soc.* **1965**, *87*, 4317–4324. (c) Frye, C. L.; Collins, W. T. *J. Am. Chem. Soc.* **1970**, *92*, 5586–5588. (d) Hossain, M. A.; Hursthouse, M. B.; Malik, K. M. A. *Acta Crystallogr.* **1979**, *B35*, 2258–2260. (e) Clegg, W.; Sheldrick, G. M.; Vater, N. *Acta Crystallogr.* **1980**, *B36*, 3162–3164. (f) Smolin, Y. I. In *Soluble Silicates*; Falcone, J. S., Ed.; ACS Symposium Series 194; American Chemical Society: Washington, DC, 1982; pp 328–348. (g) Day, V. W.; Klemperer, W. G.; Mainz, V. V.; Millar, D. M. *J. Am. Chem. Soc.* **1985**, *107*, 8262–8264. (h) Feher, F. J.; Budzichowski, T. A. *J. Organomet. Chem.* **1989**, *373*, 153–163.
(16) For example, we have recently completed an analysis of the vibrational spectra of several $R_8Si_8O_{12}$ species. Manuscript in preparation.
(17) Although the silsesquioxane analogues of tetrahedrane ($R_4Si_4O_6$)[15a] and prismane ($R_6Si_6O_9$)[15f,18] have been prepared, neither the T_6O_9 core nor the T_4O_6 core has been observed in zeolites.
(18) Feher, F. J.; Newman, D. A.; Walzer, J. F. *J. Am. Chem. Soc.* **1989**, *111*, 1741–1748.
(19) Available from QCPE, Creative Arts Building 181, Indiana University, Bloomington, IN 47405.
(20) For Si parameters, see: Dewar, M. J. S.; Jie, C. *Organometallics* **1987**, *6*, 1486–1490. For Al parameters, see: Dewar, M. J. S.; Holder, A. J. *Organometallics* **1990**, *9*, 508–511.
(21) (a) McIver, J. W.; Komornicki, A. *Chem. Phys. Lett.* **1971**, *10*, 303–306. (b) McIver, J. W.; Komornicki, A. *J. Am. Chem. Soc.* **1972**, *94*, 2625–2633.
(22) Armstrong, D. R.; Perkins, P. G.; Stewart, J. J. P. *J. Chem. Soc., Dalton Trans.* **1973**, 838–840.
(23) For example, recent *ab initio* calculations at the 6-31G(d) level predict the Si–O–Si angle to be 26° too large. To obtain a more accurate calculated bond angle, calculations explicitly including the effects of electron correlation had to be performed. Shambayati, S.; Blake, J. F.; Wierschke, S. G.; Jorgensen, W. L.; Schreiber, S. L. *J. Am. Chem. Soc.* **1990**, *112*, 697–703.
(24) Feher, F. J.; Budzichowski, T. A.; Weller, K. J. *J. Am. Chem. Soc.* **1989**, *111*, 7288–7289.

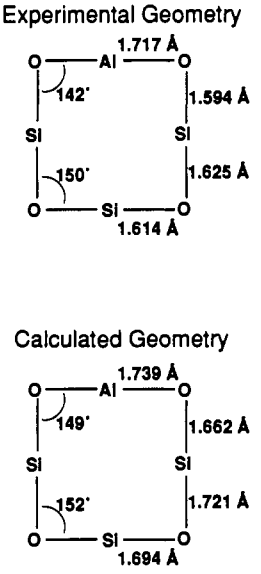

Figure 2. Comparison of experimental and calculated geometry of the $AlSi_3O_4$ face of aluminosilicate cubes. Bond distances and angles given are average values. The experimental geometry for $(Ph_3PO)Cy_7AlSi_7O_{12}$ was taken from ref 24. Calculated geometry for $(HO)_8AlSi_7O_{12}^-$ was used.

Table II. Experimental and Calculated Si–O Bond Lengths in $R_8AlSi_7O_{12}$ as a Function of Distance from Aluminum

		calcd[d]		
n[a]	exptl[b,c]	R = H	R = OH	
1	1.594 (0.001)	1.671	1.662	short
2	1.625 (0.006)	1.728	1.721	long
3	1.614 (0.004)	1.702	1.694	short
4	1.619 (0.003)	1.720	1.713	long
5	1.615 (0.007)	1.709	1.701	
$\bar{x}$[e]	1.615	1.709	1.701	

[a] n is the number of bonds away from the aluminum center where n = 0 corresponds to the Al–O bond. [b] Experimental data for $(Ph_3PO)(cy)_7AlSi_7O_{12}$ from Feher, F. J.; Budzichowski, T. A.; Weller, K. J. *J. Am. Chem. Soc.* **1989**, *111*, 7288–7289. [c] Values in parentheses are the maximum deviations from the average values given. [d] This work. [e] Average (weighted) Si–O bond length.

$(HO)_8AlSi_7O_{12}^-$ were consistently too long, as found for the silicates discussed above. Si–OSi bond lengths ranged from 1.690 to 1.728 Å while the Si–OAl bonds ranged from 1.658 to 1.667 Å. The calculated Al–O bond lengths (1.736–1.744 Å) were again found to be somewhat too long, although the magnitude of this error was somewhat smaller than the error in the Si–O bond lengths. Calculated results for $H_8AlSi_7O_{12}^-$ were similar with Si–OSi bond lengths ranging from 1.702 to 1.728 Å, Si–OAl bond lengths averaging 1.671 Å, and Al–OSi bond lengths averaging 1.743 Å.

Figure 2 summarizes these results for $R_8AlSi_7O_{12}$ by comparing the average geometry on faces of these cubes for both the experimental and calculated structures. An intriguing feature of the observed X-ray structure is the alternation between "long" and "short" Si–O bond lengths as one goes around the ring. This effect is most pronounced nearest the Al center and decreases in magnitude as the distance from this atom increases. The calculated geometry also shows this same type of bond alternation.[25] The experimental and calculated bond lengths as a function of the number of bonds away from the aluminum center are presented in Table II.[26]

(25) To verify that the calculated geometry was not fortuitously reproducing this feature as a consequence of the initial geometry, an additional calculation was performed where this type of bond alternation was rigorously avoided in the starting geometry. The optimized geometry obtained from this calculation was virtually identical with the original calculated geometry.

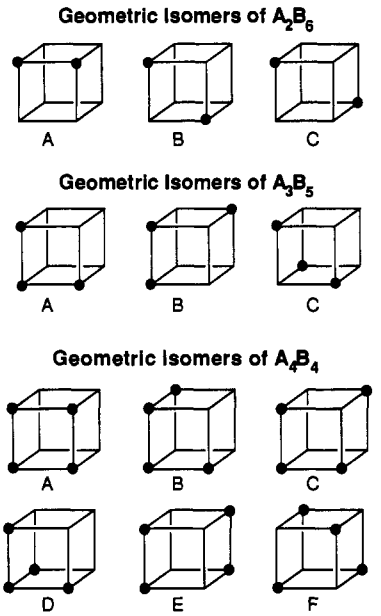

Figure 3. Schematic illustration of the structural isomers of $R_8Al_xSi_{8-x}O_{12}^{x-}$. Aluminum and silicon occupy the eight corners of the cubes while the bridging oxygen atoms (not shown) lie on each of the 12 edges. The eight "R" groups (also not shown) cap each corner. Dark spheres represent sites occupied by aluminum atoms.

The bond alternation observed in the aluminosilicate system is not unique and has been observed, for example, in certain metal oxide systems.[27] However, the aluminosilicate systems do differ from the metal oxide systems in that the bond alternation cannot be based on a "trans" effect of the heavy atom centers since the bond angles around each of the Al and Si centers all lie within a few degrees of the ideal tetrahedral angles. Insight into this effect is provided by the calculated bond orders. The calculated bond orders parallel the trends in bond length, with long bonds calculated as being weaker than short bonds, and for each silicon the sum of the three Si–O bond orders is approximately constant. The three silicon atoms nearest the aluminum center each contain both the strongest Si–O bond (Si–OAl) and two of the weakest Si–O bonds. These weakly bound oxygen atoms are connected to three silicon atoms by relatively strong Si–O bonds. Consequently, the remaining Si–O bonds on these silicon atoms are somewhat weak. Finally, these three somewhat weakly bound oxygen atoms link this second set of silicon atoms to the single silicon furthest from aluminum, which has three equivalent Si–O bonds.

The ability of the calculated geometries to so successfully reproduce experimental results indicates that these calculations, while not highly accurate in an absolute sense, are quite successful at predicting even rather subtle trends and can be highly useful when used in a comparative manner.

Relative Isomer Stability. One of the goals of this work is to determine if semiempirical calculations on molecular species can be used to provide insights into the thermodynamics of substitution patterns in solid-state structures. The most studied and well-understood rule relating to substitution patterns in zeolites is Loewenstein's rule,[3] which states that two tetrahedrally-coordinated aluminum centers will not reside adjacent to each other if connected by a single bridging oxygen atom. Octanuclear silsesquioxanes and aluminosilsesquioxanes were initially chosen for this study to provide a clear test of whether or not semiempirical

(26) The magnitude of this bond alternation is larger and more consistent in the calculated geometry than observed in the experimental structure. While part of this is probably due to inaccuracies of the calculational method, it should also be realized that the calculations are performed on isolated molecules (i.e. gas phase) at 0 K. The experimental structure may be affected by packing forces in the crystalline lattice and thermal motion.

(27) Che, T. M.; Day, V. W.; Francesconi, L. C.; Fredrich, M. F.; Klemperer, W. G.; Shum, W. *Inorg. Chem.* **1985**, *24*, 4055–4062.

Table III. Calculated Heats of Formation (kcal/mol) for $R_8Al_xSi_{8-x}O_{12}^{x-}$ Cubes

		R = H		R = OH	
x	isomer	ΔH_f	$\Delta\Delta H_f$[a]	ΔH_f	$\Delta\Delta H_f$[a]
0		-1145.9		-1770.4	
1		-1160.9		-1785.2	
2	A	-1098.6	14.9	-1726.3	14.7
2	B	-1108.9	4.6	-1736.4	4.6
2	C	-1113.5	0.0	-1741.0	0.0
3	A	-969.2	19.9	-1603.6	17.5
3	B	-983.7	5.4	-1617.0	4.1
3	C	-989.1	0.0	-1621.1	0.0
4	A	-761.2	39.6	-1405.3	35.9
4	B	-775.8	25.0	-1418.9	22.3
4	C	-785.6	15.2	-1428.5	12.7
4	D	-771.0	29.8	-1412.8	28.4
4	E	-790.2	10.6	-1432.6	8.6
4	F	-800.8	0.0	-1441.2	0.0

[a] Relative heat of formation compared to most stable isomer.

calculations can properly estimate the relative stability of geometric isomers. Since there do not appear to be any known violations of Loewenstein's rule, failure of these calculations to correctly predict the relative stability of these isomers would have indicated a severe limitation of this model. Calculations were performed on the molecules $R_8Si_8O_{12}$, $R_8AlSi_7O_{12}^-$, $R_8Al_2Si_6O_{12}^{2-}$ (three isomers), $R_8Al_3Si_5O_{12}^{3-}$ (three isomers), and $R_8Al_4Si_4O_{12}^{4-}$ (six isomers), which are shown schematically in Figure 3.[28] For each molecular formula, the most thermodynamically stable isomer should have the lowest (most negative) calculated heat of formation. It should be obvious that the results of these calculations can only be related to solid-state structures if the T_8O_{12} core is relatively unaffected by substitution on the corners of each cube (different "R" groups). However, it was noted above for octasilsesquioxanes that different R groups did give rise to small changes in the geometries of these cubes. In order to determine the thermodynamic effects of different "capping" groups, calculations were performed for each isomer using both H and OH as the R groups. The results are summarized in Table III.

For $R_8Si_8O_{12}$ and $R_8AlSi_7O_{12}^-$, only one isomer of each is possible. For $R_8Al_2Si_6O_{12}^{2-}$, three isomers are possible. One isomer (A) contains an Al–O–Al linkage and is thus expected to be the least stable since the remaining two isomers both satisfy Loewenstein's rule. However, the isomer where the aluminum atoms were arranged on opposite corners of the cube (isomer C) does not contain any Al–O–Si–O–Al linkages, so Dempsey's rule would predict that this isomer should be most stable. For $R_8Al_3Si_5O_{12}^{3-}$ and $R_8Al_4Si_4O_{12}^{4-}$, only one isomer of each (isomers C and F, respectively) does not contain any Al–O–Al linkages. Therefore, these isomers are predicted to be the most stable.

The calculated results are in excellent agreement with the above predictions. In all cases where two or more aluminum atoms are present, the most stable isomer was calculated to be the one in which the Al atoms are situated as far away from each other as possible. This is also the expected result based on a simple electrostatic repulsion model where $RSiO_{3/2}$ is formally replaced by $RAlO_{3/2}^-$. Although the absolute magnitude of the calculated relative stability for each set of isomers changes slightly, the trends are the same for both R = H and R = OH, suggesting that the capping group plays only a secondary role. Although it would be difficult to conclude that the calculated heats of formation for the molecular species included in this study can be applied in a qualitative sense to solid-state silicates and aluminosilicates, the relative stabilities do correlate in the expected manner. It should be noted that the calculated heats of formation for the $R_8Al_4Si_4O_{12}^{4-}$ isomers are considered to be somewhat less accurate than the other vlaues reported because the highest occupied orbitals were calculated to be positive. This type of behavior has been observed in other work on highly anionic species[7c] and is a result of the large negative charge of the compounds examined and the limited basis sets used in these types of calculations.[29]

(28) Only geometric isomers are included. Optical isomers were not considered since they should not differ in energy.

Table IV. Calculated Energies for $(H)H_8Al_xSi_{8-x}O_{12}^{1-x}$

x	ΔH_f, kcal/mol	$\Delta\Delta H_f$, kcal/mol[a]	isomer type
0	-1005.5	140.4	Si–O(H)–Si
1	-1115.3	45.6	Al–O(H)–Si
1	-1094.0	66.9	Al–O–Si–O(H)–Si
1	-1085.5	75.4	Al–O–Si–O–Si–O(H)–Si
2C	-1133.8	-20.3	Al–O(H)–Si
2C	-1121.0	-7.5	Al–O–Si–O(H)–Si

[a] $\Delta\Delta H_f$ = energy difference between protonated and deprotonated forms.

Protonation Studies. One advantage of computational studies is the high degree of control one has over the chemistry to be examined. This feature was exploited in an examination of the site preference for protonation of octanuclear silsesquioxanes and heterosilsesquioxanes. Three molecules were chosen for examination, $H_8Si_8O_{12}$, $H_8AlSi_7O_{12}^-$, and the "C" (most stable) isomer of $H_8Al_2Si_6O_{12}^{2-}$. In all cases, protonation was assumed to occur on a bridging oxygen atom. For the aluminosilicates, more than one protonation site is possible based on proximity to the aluminum atom(s). Only single protonations were included in this study. Examination of the effects of multiple protonation are currently under investigation.

In all cases, protonation was calculated to cause an increase in the T–O(H)T (T = Si, Al) bond length and a bond alternation similar to that observed for $R_8AlSi_7O_{12}^-$. The calculated heats of formation are listed in Table IV. The $\Delta\Delta H_f$ values given are simply the differences between the calculated heats of formation of the protonated and unprotonated forms and are not the heats of protonation. In all cases, the most stable (least acidic) protonation sites were found to be those oxygens directly bound to aluminum centers, which is consistent with a simple electrostatic interpretation. Substitution of Si^{IV} with Al^{III} results in an increase in negative charge on the oxygen atoms directly bound to aluminum, which should make these the preferred protonation sites. While the electrostatic model is successful, the difference in protonation at Al–O–Si–O(H)–Si vs Al–O–Si–O–Si–O(H)–Si sites suggest that this is an oversimplification and that the charge is not completely localized. Bond alternation has been suggested[27] as one means by which charge can be delocalized and may at least partially explain this effect.

In all cases, the most stable protonation site was determined based on the relative stability of the protonated isomers. The calculated atomic charges in the unprotonated forms *did not* uniformly predict the oxygen atoms bound to aluminum to be the most negatively charged. The calculated partial charges of the acidic hydrogen atom have also been suggested[30] as an indicator of acid strength. Although the atomic charges calculated in this work did consistently predict that the acidic proton attached to the oxygen atom bridging aluminum and silicon should be the least acidic (smallest positive charge), the calculated charge for the two remaining protonation sites in $(H)H_8AlSi_7O_{12}$ predicted the Al–O–Si–O(H)-Si proton to be the most acidic, in variance with the results predicted on the basis of the relative heats of formation. While these results may be an artifact of the method used (perhaps most importantly, the limited basis set employed), it does suggest that one must be very careful about predicting oxygen atom basicity based solely on calculated partial charges. This is particularly true in situations where there is delocalization of charge and the absolute differences in partial charges between atoms are calculated (as expected) to be small.

In all of the work discussed above, protonation of the cubes was assumed to occur on the outside of the cube. While the dimensions of the T_8O_{12} cube are too small to allow inclusion of small organic

(29) Alrich, R. *Chem. Phys. Lett.* **1975**, *34*, 570–574.
(30) (a) Kazansky, V. B.; Gritscov, A. M.; Andreeve, V. M.; Zhidomirov, G. M. *J. Mol. Catal.* **1978**, *4*, 135–149. (b) O'Malley, P. J.; Dwyer, J. *J. Phys. Chem.* **1988**, *92*, 3005–3007.

molecules, it is quite conceivable that a proton could fit inside one of these cubes.[31] To examine this possibility, calculations were performed on the species $(H)H_8Si_8O_{12}^+$ where the proton was placed on the inside of the cube. A stationary point was found where the proton was attached to a bridging oxygen atom that had distorted such that it was pointing inside of the cube also. This type of distortion would be expected since the bridging oxygen atoms in these molecules bend away from the center of the Si_8O_{12} core, which should force the bridging oxygen electron lone pairs to be oriented away from the core. However, a force calculation on this distorted geometry yielded a single negative eigenvalue, which indicates that this was a transition state and not a true ground state.[21] This transition state was calculated to lie about 8 kcal/mol higher in energy than the minima found where protonation occurred on the outside of the cube.

Conclusion

This work has shown that semiempirical calculations can be successfully applied to molecular aluminosilicates to predict geometries and relative stabilities of geometric isomers. While the calculated Si-O bond lengths are consistently longer than the experimental values, the errors were found to be reasonably constant (ca. +0.10 Å) and size-independent, which allows even rather subtle trends to be successfully predicted. The relative stability of geometric isomers of the general formula $R_8Al_xSi_{8-x}O_{12}^{x-}$ were calculated and found to be in agreement with Loewenstein's rule, suggesting that these systems may be used to successfully study certain properties of zeolites. Protonation studies on these molecules suggest, as expected, that protonation occurs preferentially at bridging oxygen atoms adjacent to aluminum. Further studies are currently in progress to model organic transformations on these molecules and to examine larger systems.

Acknowledgment. This work was supported by research grants from the University of Missouri—Kansas City. The calculations were performed on the University's DEC VAX 6460 computer. We are grateful to Prof. Andrew Holder for many helpful suggestions on running these programs.

Supplementary Material Available: Complete tables of Cartesian coordinates at the optimized geometries and calculated atomic charges for all molecules included in this study (34 pages). Ordering information is given on any current masthead page.

(31) The body diagonal of these cubes is ca. 5.3 Å.

Contribution from the Department of Chemistry, University of Mississippi, University, Mississippi 38677, and School of Chemistry and Molecular Sciences, University of Sussex, Falmer, Brighton BN1 9QJ, England

Electrochemical and Spectroscopic Characterization of $\{Nb_6Cl_{12}\}^{z+}$ Chloride Clusters in the Aluminum Chloride–1-Methyl-3-ethylimidazolium Chloride Molten Salt

Robert Quigley,[1,2] Paul A. Barnard,[3] Charles L. Hussey,*[,3] and Kenneth R. Seddon[1]

Received September 5, 1991

The electrochemistry and electronic absorption spectroscopy of metal-metal-bonded chloride clusters derived from the $\{Nb_6Cl_{12}\}^{z+}$ (z = 1–4) cores were investigated in the room-temperature molten salt aluminum(III) chloride–1-methyl-3-ethylimidazolium chloride ($AlCl_3$–MeEtimCl). Anionic complexes of this core cluster of the type $[(Nb_6Cl_{12})Cl_6]^{(6-z)-}$ were identified in basic melt. Reversible electrode reactions with $E_{1/2}$ values of −0.02 and 0.39 V versus the Al^{3+}/Al couple in the 66.7/33.3 mol % $AlCl_3$–MeEtimCl melt at 100 °C were found for the oxidation of the chloride complexes derived from the $\{Nb_6Cl_{12}\}^{2+}$ and $\{Nb_6Cl_{12}\}^{3+}$ cores, respectively. The overall redox scheme for these complexes is

$$[(Nb_6Cl_{12})Cl_6]^{5-}? \underset{+e^-}{\overset{-e^-}{\rightleftharpoons}} [(Nb_6Cl_{12})Cl_6]^{4-} \underset{+e^-}{\overset{-e^-}{\rightleftharpoons}} [(Nb_6Cl_{12})Cl_6]^{3-} \underset{+e^-}{\overset{-e^-}{\rightleftharpoons}} [(Nb_6Cl_{12})Cl_6]^{2-}$$

$[(Nb_6Cl_{12})Cl_6]^{5-}$ is moderately stable on the voltammetric time scale but decomposes during controlled-potential electrolytic reduction of the parent species. Likewise, $[(Nb_6Cl_{12})Cl_6]^{2-}$ is voltammetrically stable, but bulk solutions of this complex are slowly reduced to $[(Nb_6Cl_{12})Cl_6]^{3-}$ by chloride ion in basic melt. Reversible electrochemical reactions involving the $\{Nb_6Cl_{12}\}^{2+/3+}$ and $\{Nb_6Cl_{12}\}^{3+/4+}$ redox systems were also found in acidic melt at 1.13 and 1.50 V, respectively, and solutes containing the $\{Nb_6Cl_{12}\}^{z+}$ (z = 2–4) cores exhibited long-term stability. The approximate 1-V positive shift in the $E_{1/2}$ values for these redox reactions in acidic melt relative to the $E_{1/2}$ values found in basic melt suggests that as many as six of the labile chloride ions that are associated with the $[(Nb_6Cl_{12})Cl_6]^{(6-z)-}$ clusters in basic melt may be replaced by $[AlCl_4]^-$ ions when these clusters are dissolved in acidic melt. The Stokes–Einstein products of the niobium clusters in both acidic and basic melts are essentially independent of the oxidation level of the core. The average values of these products are 8.2×10^{-11} (40 °C) and 1.2×10^{-10} (100 °C) g cm s^{-2} K^{-1}, respectively.

Introduction

The combination of aluminum(III) chloride and certain quaternary organic chloride salts with "bulky" cations, notably 1-(1-butyl)pyridinium chloride (BupyCl) and 1-methyl-3-ethylimidazolium chloride (MeEtimCl), results in ionic liquids or molten salts that are fluids at room temperature. Several reviews covering various aspects of these room-temperature chloroaluminate melts are available.[4] The Lewis acidity of these molten salts can be varied over a large range by simply altering the $AlCl_3$ content of the mixture. This adjustable acidity leads to a family of solvents with vastly different properties. For example, mixtures that are greater than 50 mol % in $AlCl_3$ are Lewis acidic due to the presence of powerful chloride ion acceptors like $[Al_2Cl_7]^-$ and $[Al_3Cl_{10}]^-$ whereas those melts that are less than 50 mol % in $AlCl_3$ are Lewis basic because they contain chloride ion that is not covalently bound to aluminum.

Basic room-temperature chloroaluminate melts are excellent solvents for transition metal chloride complexes,[5] including the chloride complexes of heteropolyatomic transition metal clusters. The electrochemistry and electronic absorption spectroscopy of several of these clusters have been investigated in these ionic solvents. Among the species that have been studied to date are $[Mo_2Cl_8]^{4-}$,[6] $[(Mo_6Cl_8)Cl_6]^{2-}$,[7] $[Re_2Cl_8]^{2-}$,[8] $[Re_2Cl_8]^{3-}$,[9] $[Re_2$-

(1) University of Sussex.
(2) Visiting scholar at the University of Mississippi.
(3) University of Mississippi.
(4) Reviews: (a) Chum, H. L.; Osteryoung, R. A. In *Ionic Liquids*; Inman, D., Lovering, D. G., Eds.; Plenum: New York, 1981; pp 407–423. (b) Hussey, C. L. In *Advances in Molten Salt Chemistry*; Mamantov, G., Mamantov, C. B., Eds.; Elsevier: Amsterdam, 1983; Vol. 5, pp 185–230. (c) Gale, R. J.; Osteryoung, R. A. In *Molten Salt Techniques*; Lovering, D. G., Gale, R. J., Eds.; Plenum: New York, 1983; Vol. 1, pp 55–78.
(5) (a) Appleby, D.; Hussey, C. L.; Seddon, K. R.; Turp, J. E. *Nature* **1986**, *323*, 614. (b) Hussey, C. L. *Pure Appl. Chem.* **1988**, *60*, 1763.
(6) Carlin, R. T.; Osteryoung, R. A. *Inorg. Chem.* **1988**, *27*, 1482.
(7) Barnard, P. A.; Sun, I-W.; Hussey, C. L. *Inorg. Chem.* **1990**, *29*, 3670.
(8) Strubinger, S. K. D.; Sun, I-W.; Cleland, W. E.; Hussey, C. L. *Inorg. Chem.* **1990**, *29*, 993.

0020-1669/92/1331-1255$03.00/0